 DOI: 10.1002/masy.201050203

Fundamentals of RAFT Miniemulsion Polymerization Kinetics

*Hidetaka Tobita**

Summary: The polymerization rate of RAFT-mediated miniemulsion polymerization, in which the time fraction of active radical ϕ_A is larger than a few percent, basically increases with reducing the particle size. For smaller particle sizes, however, the statistical variation of monomer concentration among particles may slow down the polymerization rate. The rate retardation by increasing the RAFT concentration occurs with or without the intermediate termination in a zero-one system. According to the present theoretical investigation, smaller particles are advantageous in implementing a faster polymerization rate, a narrower MWD, and a smaller number of dead polymer chains.

Keywords: kinetics (polym.); miniemulsion polymerization; molecular weight distribution/molar mass distribution; particle size; reversible addition fragmentation chain transfer (RAFT)

Introduction

Recently, the controlled/living radical polymerization (CLRP) has attracted much attention as a novel method to synthesize well-defined polymers. There are several different types of CLRP systems. The time fraction of the active radical period ϕ_A, is extremely small for the stable free radical mediated polymerization (SFRP) and for the atom transfer radical polymerization (ATRP). On the other hand, the ϕ_A-value does not have to be small for the reversible addition-fragmentation chain transfer (RAFT) polymerization, and ϕ_A is close to unity in the degenerative transfer (DT) polymerization.

For the conventional emulsion polymerization in which $\phi_A = 1$, high MW polymers can be produced with a high polymerization rate, by physically isolating polymer radicals into separate polymer particles to suppress bimolecular termination reactions. For CLRP, the effect of particle size on the polymerization rate was theoretically discussed by Butte et al.,[1,2] Charluex,[3] Zetterlund et al.[4–7] and Tobita et al.[8–11]

In this article, the effects of small reaction locus on the polymerization rate and MWD are highlighted for the RAFT polymerization with $\phi_A >$ ca. 0.1, based on the Monte Carlo simulation results.

Polymerization Mechanism

The essence of RAFT-mediated free radical polymerization resides in the following reversible reaction:

$$\mathrm{R}_i^{\bullet} + \mathrm{XP}_j \underset{k_1}{\overset{k_2}{\rightleftharpoons}} \mathrm{P}_i\mathrm{XP}_j \underset{k_2}{\overset{k_1}{\rightleftharpoons}} \mathrm{P}_i\mathrm{X} + \mathrm{R}_j^{\bullet} \qquad K \equiv \frac{k_1}{k_2}[\mathrm{mol}\cdot\mathrm{L}^{-1}] \tag{1}$$

where P_i is the polymer with chain length i, and $R_i^{\bullet}$ is the active polymer radical with chain length i. Note that the intermediate PXP is a radical, but normally its activity is not very high and the propagation reaction of PXP can be neglected.

If the k_1-value is large enough and the reaction is considered as a simple chain transfer reaction, as the name RAFT

Department of Materials Science and Engineering, University of Fukui, 3-9-1 Bunkyo, Fukui 910-8507, Japan
E-mail: tobita@matse.u-fukui.ac.jp

implies, the polymerization rate does not change by the RAFT reaction. On the other hand, the rate retardation by increasing the RAFT concentration has been observed experimentally both in bulk[12,13] and miniemulsion[14] polymerization. To elucidate the retardation behavior that cannot occur simply with chain transfer reaction, two different types of models were proposed. One type of model[12] that assumes a cross-termination between propagating radical, $R^{\bullet}$ and the adduct radical, PXP. This intermediate termination model usually leads to a relatively large *K*-value. On the other hand, another model assumes a slow fragmentation of PXP, with a small *K*-value.[13] There is an ongoing discussion on this problem.[15] In this article, the cases with a relatively large *K*-values, whose magnitude is a similar order of the RAFT concentration, [XP], are considered.

Table 1 shows the kinetic parameters used in the present article. In the table, k_{ct} is the rate constant for the intermediate termination. The initial monomer concentration is set to be $[M]_0 = 8$ mol/L, and the initial RAFT concentrations considered are $[XP]_0 = 4 \times 10^{-3}$ and 4×10^{-2} mol/L. To simplify the discussion, the initial RAFT agent and the polymeric RAFT are not distinguished, and the pre-equilibrium kinetics[13] are not considered in this article.

The time fraction of active radical period, ϕ_A is given by:[10,16]

$$\phi_A = \frac{\bar{t}_{R^{\bullet}}}{\bar{t}_{R^{\bullet}} + \bar{t}_{PXP}} = \frac{K}{K + [XP]} \quad (2)$$

In the present investigation, $K = 0.01$, and therefore, the cases with $\phi_A >$ ca. 0.2 are considered.

Figure 1 illustrates the chain growth process of RAFT polymerization. In the RAFT polymerization, once a radical is generated, it is always terminated after forming a single kinetic chain, schematically connected by the dotted lines in Figure 1. The pseudo-livingness results from the fact that an active radical is relayed to a large number of chains before finally being stopped by a bimolecular termination reaction. When the ϕ_A-value is large, the polymerization rate, R_p is given by:

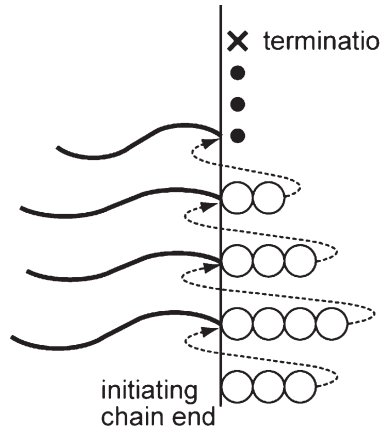

Figure 1.
Schematic representation of the chain formation process.

$$R_p = R_I \nu \quad (\text{for } \phi_A > \text{ca. } 0.1) \quad (3)$$

where R_I is the initiation rate, and ν is the kinetic chain length, with $\nu = k_p[M]/k_t[R^{\bullet}]$ for $k_{ct} = 0$, and $\nu = k_p[M]/(k_t[R^{\bullet}] + 2k_{ct}[PXP])$ for $k_{ct} \neq 0$. Obviously, Equation (3) conforms to $R_p = k_p[M][R^{\bullet}]$ with the relationship, $R_I = R_t$.

Figure 2 shows the calculated conversion development for bulk polymerization. For $k_{ct} = 0$, the polymerization rate does not change even when the RAFT concentration is increased, because the kinetic chain length ν is not changed by the chain transfer reaction. On the other hand, with $k_{ct} \neq 0$, the polymerization rate is reduced by the decrease in $\nu = k_p[M]/(k_t[R^{\bullet}] + 2k_{ct}[PXP])$.

Table 1.
Rate constants used in the simulation.

k_1 [s^{-1}]	k_2 [$L \cdot mol^{-1} \cdot s^{-1}$]	k_p [$L \cdot mol^{-1} \cdot s^{-1}$]	k_t [$L \cdot mol^{-1} \cdot s^{-1}$]	k_{ct} [$L \cdot mol^{-1} \cdot s^{-1}$]
1×10^4	1×10^6	500	1×10^7	0, 1×10^7

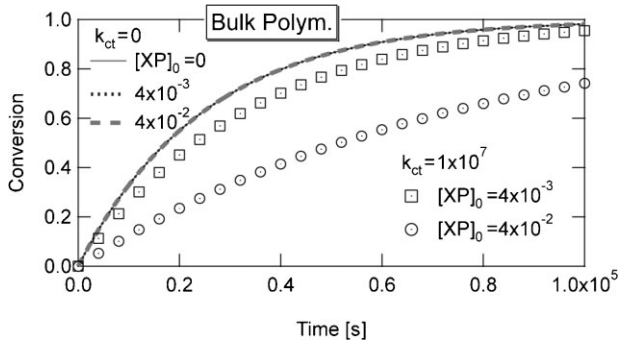

Figure 2.
Calculated conversion development for bulk polymerization.

In emulsion polymerization, the kinetic chain length can be made larger by isolating radicals in each particle, and the polymerization rate increases by reducing the particle size.[1,2,8,10]

On the other hand, when $\phi_A \ll 1$, the polymerization rate is given by the following equation, as in the case of SFRP.[9,17]

$$R_p = k_1[\mathrm{PXP}]\overline{P}_{n,SA} \qquad (\text{for } \phi_A \ll 1) \qquad (4)$$

where $\overline{P}_{n,SA}$ is the average number of monomeric units added during a single active period, which is given by:[9,17]

$$\overline{P}_{n,SA} = k_p[\mathrm{M}]\bar{t}_{R\bullet} = \frac{k_p[\mathrm{M}]}{k_2[\mathrm{XP}]} \qquad (5)$$

Because [PXP] and [XP] are essentially the same as in bulk polymerization, and therefore, the polymerization rate does not increase by reducing the particle size, for a constant monomer/initiator ratio.[8,17] Miniemulsion polymerization experiment is an easy method to examine whether the *K*-value is large or not.

Simulation Method for Miniemulsion Polymerization

The Monte Carlo (MC) simulation algorithm proposed earlier[10,11] is used for the miniemulsion polymerization. Each polymer particle is considered as an isolated microreactor with a given diameter, D_p. The exit of radicals and monomer transfer among particles are neglected. It is assumed that the radicals are generated in the water phase and enter each polymer particle one by one. In order to investigate the effect of particle size, the monomer/initiator ratio is kept constant. The radical generation rate is chosen to make the average time interval between radical entry is $\bar{t}_e = 50\,\mathrm{s}$ for $D_p = 100\,\mathrm{nm}$. This condition corresponds to the initiation rate in bulk polymerization $R_I = 6.366 \times 10^{-8}\,\mathrm{mol \cdot L^{-1} \cdot s^{-1}}$. Table 2 shows the average time interval between radical entry $\bar{t}_e$ for different D_p-values, which can be calculated from:

$$\bar{t}_e = \left(R_I V_p N_A\right)^{-1} \qquad (6)$$

where V_p is the volume of a particle given by $V_p = \pi D_p^3 \big/ 6$, and N_A is the Avogadro constant. The $\bar{t}_e$-value is large when the particle size is small, as show in Table 2.

Retardation in Emulsified Systems

Figure 3 shows the MC simulation results for miniemulsion polymerization with $D_p = 50\,\mathrm{nm}$. Compared with bulk polymerization shown in Figure 2, two important characteristics must be pointed out. First, the rate retardation by increasing the

Table 2.
Average time interval between radical entry to a particle.

D_p [nm]	30	50	100	150	300
$\bar{t}_e$ [s]	1852	400	50	14.8	1.85

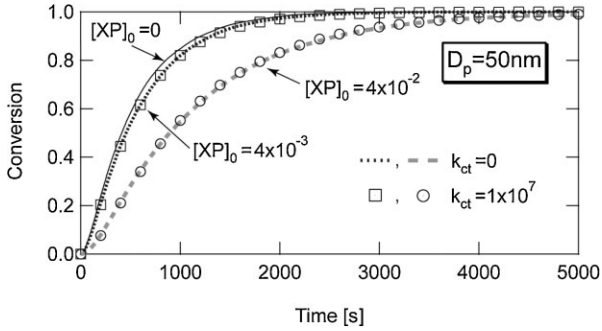

Figure 3.
MC simulation results for the conversion development with and without intermediate termination for $D_p = 50$ nm.

RAFT concentration is observed without contribution of the intermediate termination. Second, the intermediate termination does not change the polymerization rate. These two features can be rationalized as follows.

From the MC simulation data, it was confirmed that the miniemulsion polymerization with $D_p = 50$ nm conforms to the zero-one kinetics,[18] i.e., the time fraction in which more than one radical exists in a particle can be neglected. Similarly with Equation (3), the polymerization rate for the zero-one system without radical exit is given by:

$$R_p = \frac{R_I \nu}{2} \tag{7}$$

The factor 2 is needed, because one half of the generated radicals start to form polymer chains while the rest are simply used to terminate the polymer chains.

For the present reaction system, the kinetic chain length ν, i.e., the average number of monomeric units consumed by the first radical until finally terminated by the second radical, is given by:

$$\nu = k_p[\mathrm{M}]\bar{t}_e\phi_A \tag{8}$$

In Equation (8), $k_p[\mathrm{M}]$ is the number of monomeric unit added to a single radical per second. The first radical grows until the entry of second radical, whose average time interval is $\bar{t}_e$. During this time interval, the radical takes two forms, $\mathrm{R}^\bullet$ and PXP. The radical can add monomeric units only when it takes the form, $\mathrm{R}^\bullet$ whose time fraction is ϕ_A.

Obviously, Equations (7) and (8) leads to Equation (9) by using the relationship given by Equation (6).

$$R_p = k_p[\mathrm{M}]\frac{0.5\phi_A}{V_p N_A} \tag{9}$$

Note that in a RAFT polymerization, a radical takes two different states, $\mathrm{R}^\bullet$ and PXP. In this article, the sum of the numbers of $\mathrm{R}^\bullet$ and PXP in a particle is represented by n, i.e.:

$$n = n_{\mathrm{R}^\bullet} + n_{\mathrm{PXP}} \tag{10}$$

In the zero-one system without the radical exit, the average of n, $\overline{n} = 0.5$, and 0.5 in Equation (9) represents the $\overline{n}$-value.

The reason for causing the rate retardation by increasing the RAFT concentration without contribution of k_{ct} can be rationalized by the decrease in the kinetic chain length ν given by Equation (8). In Equation (8), the time fraction of active radical period, ϕ_A decreases when the RAFT concentration [XP] is increased, as represented by Equation (2). The line 1 in Figure 4 shows how ϕ_A decreases with [XP].

One may think that the ϕ_A-value must decrease also in bulk polymerization, then why doesn't the rate retardation occur without the assistance of k_{ct} in bulk? As shown in the right axis of Figure 4, the

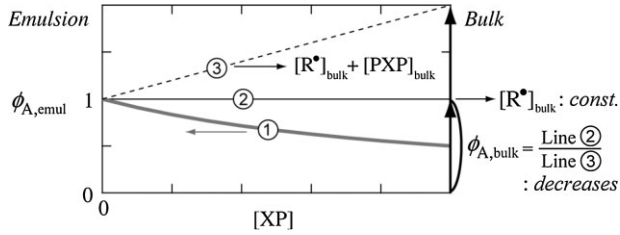

Figure 4.
Effect of RAFT concentration on ϕ_A for the zero-one miniemulsion polymerization (left), and on the active [R•] and inactive [PXP] radical concentrations in bulk polymerization for $k_{ct} = 0$ (right). For bulk polymerization, ϕ_A is represented by the ratio, (line 2)/(line 3).

active radical concentration is fixed by $[R^\bullet] = \sqrt{R_I/k_t}$, and [PXP] increases to satisfy the equilibrium relationship $k_1[PXP] = k_2[R^\bullet][XP]$. It is true that $\phi_A =$ (line 2)/(line 3) decreases with increasing [XP], but the polymerization rate does not change in bulk polymerization because $[R^\bullet]$ is unchanged. To elucidate the retardation, k_{ct} is needed.

On the other hand, for the zero-one system, the magnitude of k_{ct} is unimportant as long as the termination rate inside the particle is large enough, and k_{ct} does not change the polymerization rate. For the rest of this article, $k_{ct} = 1 \times 10^7\ \mathrm{L \cdot mol^{-1} \cdot s^{-1}}$ is used for the calculation.

Rate Reduction for Small Particles

Table 2 shows that the time interval between radical entry is $\bar{t}_e = 400$ s for $D_p = 50$ nm. The conversion-time curve in Figure 3 shows that the initial transient period to reach $\bar{n} = 0.5$ cannot be neglected. The time development of $\bar{n}$ for a zero-one system without the radical exit is given by:[10]

$$\bar{n} = e^{-t/\bar{t}_e} \sinh(t/\bar{t}_e) \tag{11}$$

Figure 5 shows a comparison with the MC simulation for $D_p = 50$ nm, which shows an excellent agreement. Note that the $\bar{n}$-development is not affected by the initial RAFT concentration for large ϕ_A's.

The conversion development of emulsion polymerization is normally given by:

$$R_p = k_p[M]\frac{\bar{n}\phi_A}{V_p N_A} \tag{12}$$

In Equation (12), ϕ_A is needed because the monomer addition occurs during that fraction of time. By substituting Equation (11) into Equation (12), the conversion development would be obtained.

Figure 6 compares Equation (12) and the MC simulation for $D_p = 50$ nm. The polymerization rate is clearly slower than that calculated from Equation (12). For the particles with $D_p > 100$ nm, such rate reduction was not observed.

Note that $[XP]_0 = 0$ corresponds to the conventional miniemulsion polymerization without using the RAFT agent. This type of rate reduction may occur for the conventional, RAFT and DT miniemulsion polymerization when the particle size D_p is smaller than, say 100 nm.

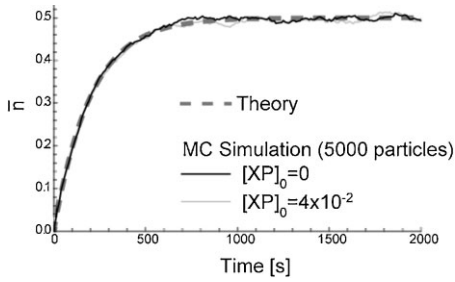

Figure 5.
Time development of $\bar{n}$ for $D_p = 50$ nm. The theoretical calculation is based on Equation (11).

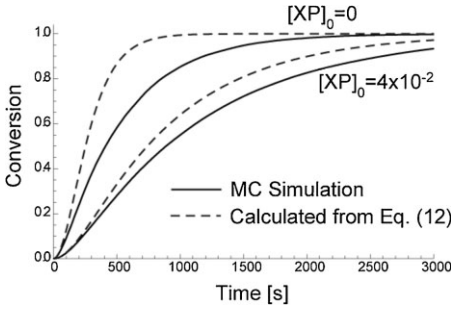

Figure 6.
Conversion development for $D_p = 50$ nm. The polymerization rate is slower than the calculation based on the average concentrations.

Monomer-Concentration-Variation (MCV) Effect

This type of rate reduction for small particles can be explained from the monomer-concentration-variation (MCV) effect.[10] Figure 7 shows the time development of conversion, x in each polymer particle for $D_p = 50$ and 100 nm, for $[XP]_0 = 0$, i.e., the conventional miniemulsion polymerization without using RAFT agent. Similar figures for the RAFT miniemulsion polymerization can be found in ref.[10] The smooth curves are the average of all particles simulated, which corresponds to the conversion-time curve that can be obtained in experiment. When the particle size is small, the statistical variation in the conversion development among particles is significant.

Equation (12) that does not agree with the MC simulation data for $D_p = 50$ nm employs the average concentrations for all the particles. When D_p is large, the use of the averages might be a reasonable approximation. However, Figure 7 clearly shows that the monomer concentration in each particle for $D_p = 50$ nm is different significantly.

Note that the monomer transfer among particles may not be neglected in real systems, depending on the types of monomer used. When the monomer is transferred from one particle to another, the monomer concentration would be equalized, and therefore, the present simulation results show the extreme cases.

As shown in Figure 7, some particles are almost dried out while other particles have not started polymerization. The radicals that exist in the particles with high conversion levels, the polymerization rate is much slower than that expected from the average monomer concentration, which may slow down the overall polymerization rate.

For the zero-one system without monomer and radical exit, the analytical solution for the conversion development that accounts for the MCV effect is given by:[10]

$$x(t) = 1 - \sum_{i=0}^{\infty} y_i(t) \tag{13}$$

$$y_{2i}(t) = \left(\frac{\lambda}{\eta}\right)^{2i} \frac{(-1)^i}{i!} e^{-\lambda t}\{U(-i, 1-2i, -\eta t) - ie^{-\eta t} U(1-i, 1-2i, \eta t)\} \quad (\text{for } i = 0,\ 1,\ 2, \ldots) \tag{14}$$

$$y_{2i+1}(t) = \left(\frac{\lambda}{\eta}\right)^{2i+1} \frac{(-1)^i}{i!} \cdot \frac{(\eta t)^{i+(1/2)}}{\sqrt{\pi}} e^{-[\lambda+(\eta/2)]t}\left\{(-1)^{i+1/2} K_{i+(1/2)}(-\eta t/2) - K_{i+(1/2)}(\eta t/2)\right\} \quad (\text{for } i = 0,\ 1,\ 2, \ldots) \tag{15}$$

Where $U(a,b,z)$ is the confluent hypergeometric function of the second kind, $K_v(z)$ is the modified Bessel function of the second kind, $\lambda \equiv 1/\bar{t}_e$ and $\eta \equiv k_p \phi_A / V_p N_A$.

Figure 8 compares the calculation of conversion x from Equations (13)–(15) and the MC simulation results. When the MCV effect is accounted for in the theory, the MC simulation results agree with the theory perfectly well. The MCV effect may need to be considered for the miniemulsion polymerization with smaller particle sizes.

The statistical variation of monomer concentration among particles may need to be accounted for in small particles, and this

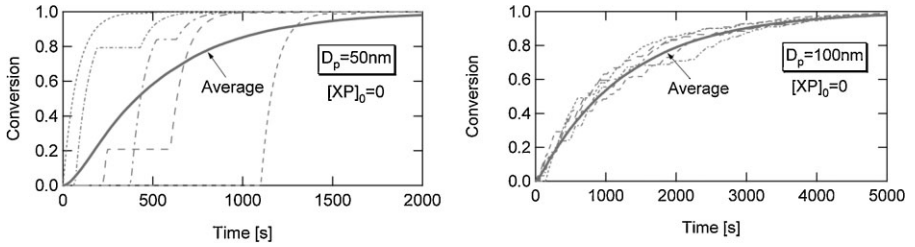

Figure 7.
Conversion development in each polymer particle obtained in the MC simulation for $D_p = 50$ and 100 nm, for $[XP]_0 = 0$.

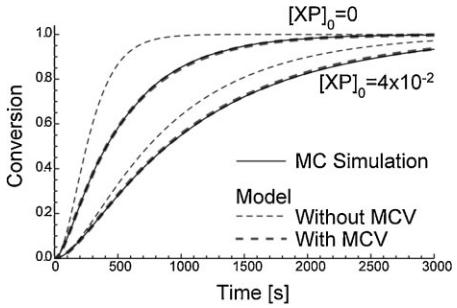

Figure 8.
Conversion development for $D_p = 50$ nm. The thin dotted curves (without MCV) are calculated from Equation (12), and the bold dotted curves (with MCV) are calculated from Equations (13)–(15). The statistical variation of monomer concentration needs to be accounted for in order to rationalize the MC simulation results.

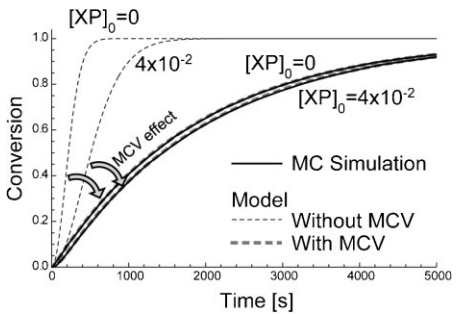

Figure 9.
Conversion development for $D_p = 30$ nm.

rate reduction effect is expected be more significant in even smaller particle cases. Figure 9 shows how significant the MCV effect is for $D_p = 30$ nm. It is interesting to note that when the rate reduction by the MCV effect is very significant, the rate retardation by increasing the RAFT concentration becomes insignificant.

Obviously, the monomer transfer among particles is expected to be more significant for smaller particles, and the present calculation results with and without MCV effect show two extreme cases. Because the rate reduction by the MCV effect is pronounced for smaller particles, the MCV effect may need to be accounted for also in the microemulsion polymerization if the monomer transfer among particles is not fast enough.

Figure 10 shows the conversion development for various particle diameters. As discussed earlier, the polymerization rate, basically, increases by reducing the particle size because of the increase in the kinetic chain length. On the other hand, because the rate reduction by the MVC effect is very significant for $D_p = 30$ nm, the polymerization rate is smaller than that for $D_p = 50$ nm in the present calculation condition.

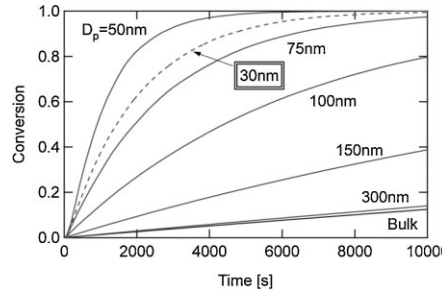

Figure 10.
Effect of particle size on the polymerization rate with $[XP]_0 = 4 \times 10^{-2}$ mol/L.

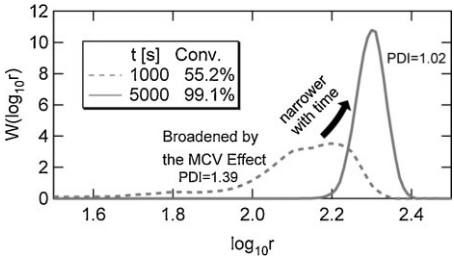

Figure 11.
Chain length distribution development during miniemulsion polymerization for $D_p = 50$ nm. $W(\log_{10} r)$ is the weight fraction distribution given as a function of the logarithm of chain length, which corresponds to the MWD usually obtained in a GPC measurement. The polydispersity index (PDI) is also shown for each distribution.

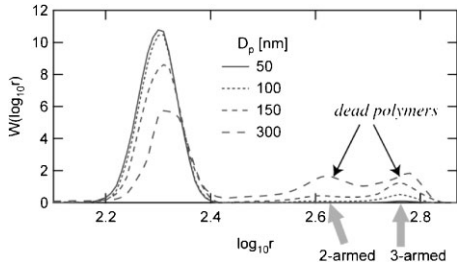

Figure 12.
Simulated chain length distribution at the final conversion levels, $x > 0.99$.

Particle Size Effects in MWD

In this section, the simulated MWD profiles for $[XP]_0 = 4 \times 10^{-2}$ mol/L is discussed. The target number-average chain length at 100% conversion is $[M]_0/[XP]_0 = 200$.

Figure 11 shows the MWD development for $D_p = 50$ nm. The MWD at $t = 1000$ s is rather broad, because of a significant MCV effect. This kind of broadening can be reduced by increasing the radical entry frequency, i.e., by reducing the $\bar{t}_e$-value.[11] On the other hand, however, larger frequencies of radical entry result in forming a larger number of dead polymer chains, and the MWD at the final conversion level becomes broader than the cases with a lower frequency of radical entry.[11] Time is a cure rather than a hasty manipulation in RAFT miniemulsion polymerization.

Figure 12 shows the effect of D_p on the formed MWD at the final conversion levels, $x > 0.99$. When the particle size is large, a significant amount of dead polymer chains are formed. Note that the combination termination is assumed in the simulation, and that an invariant termination rate constant is used throughout the polymerization. In real systems, the termination reaction is expected to be dependent on both conversion and chain length. If the termination rate coefficient becomes smaller at higher conversion levels, the amount of dead polymer chains would becomes smaller than the present MC simulation results. In addition, with the chain length dependent termination, the chain length of the dead polymer chain peaks may shift to smaller chain lengths.

Despite that simplified assumptions are used for the termination reactions, Figure 12 highlights important characteristics of RAFT miniemulsion polymerization. Smaller particles are advantageous in obtaining a narrow MWD with a smaller number of dead polymer chains.

The dead polymer chain lengths are about twice and three times as large as the main peak polymers at the final conversion level. Because the main peak keeps on moving to larger chain lengths as the polymerization proceeds, this fact shows that dead polymer chains are formed mainly at the final stages of polymerization, especially, for large D_p's. The reason for this can be rationalized as follows.

Figure 13 shows conversion developments for various D_p's. Because the polymerization

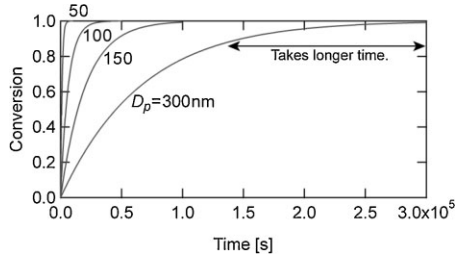

Figure 13.
Conversion development for $D_p = 50$, 100, 150 and 300 nm.

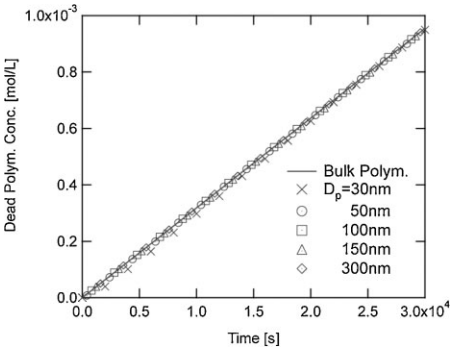

Figure 14.
Time development of the dead polymer chain concentration.

rate is slower for larger particle cases, it takes very long time to reach high conversion levels for larger D_p's. In addition, the polymerization rate becomes very slow at higher conversion levels.

Figure 14 shows how the number of dead polymer chains increases with time. The initiation and termination rates are balanced for both the bulk and miniemulsion polymerization. In the present calculations, a constant R_I is used, and the number of dead polymer chains increases linearly with time. In terms of the reaction time, a very long time is required at the final stage of polymerization, as shown in Figure 13. This is why a significant amount of dead polymer chains are formed at the final stage.

A larger number of dead polymer chains are formed for larger D_p's, simply because it takes longer time to reach a high conversion level.

The dead polymer chains are formed with time, and therefore, a faster polymerization rate is advantageous in RAFT polymerization to attain higher livingness. The polymerization rate increases by reducing the particle size, and therefore, smaller particles are advantageous both for productivity and quality of the polymers in miniemulsion RAFT polymerization.

Conclusion

According to the present theoretical investigation, smaller particles are advantageous in implementing (1) a faster polymerization rate, (2) a narrower MWD, and (3) higher livingness.

The rate retardation occurs with or without the intermediate termination in a zero-one system. Therefore, miniemulsion polymerization with a small D_p is a poor experimental technique to determine the rate constant for the intermediate termination, k_{ct}.

For smaller D_p's, the polymerization rate might be reduced by the statistical variation of the monomer concentration among particles, which is named the monomer-concentration-variation (MCV) effect. The MCV effect may need to be considered also for the conventional miniemulsion polymerization without using the RAFT agent and for the degenerative transfer (DT) miniemulsion polymerization.

[1] A. Butte, G. Storti, M. Morbidelli, *Macromolecules* **2000**, *33*, 3485.
[2] A. Butte, G. Storti, M. Morbidelli, *Macromolecules* **2001**, *34*, 5885.
[3] B. Charleux, *Macromolecules* **2000**, *33*, 5358.
[4] P. B. Zetterlund, M. Okubo, *Macromolecules* **2006**, *39*, 8959.
[5] Y. Kagawa, P. B. Zetterlund, H. Minami, M. Okubo, *Macromol. Theory Simul.* **2006**, *15*, 608.
[6] P. B. Zetterlund, M. Okubo, *Macromol. Theory Simul.* **2007**, *16*, 221.
[7] P. B. Zetterlund, Y. Kagawa, M. Okubo, *Macromolecules* **2009**, *42*, 2488.
[8] H. Tobita, F. Yanase, *Macromol. Theory Simul.* **2007**, *16*, 476.
[9] H. Tobita, *Macromol. Theory Simul.* **2007**, *16*, 810.
[10] H. Tobita, *Macromol. Theory Simul.* **2009**, *18*, 108.
[11] H. Tobita, *Macromol. Theory Simul.* **2009**, *18*, 120.
[12] M. J. Monteiro, H. de Brouwer, *Macromolecules* **2001**, *34*, 349.
[13] C. Barner-Kowollik, J. F. Quinn, T. L. U. Nguyen, J. P. A. Heuts, T. P. Davis, *Macromolecules* **2001**, *34*, 7849.
[14] Y. Luo, R. Wang, L. Yang, B. Yu, B. Li, S. Zhu, *Macromolecules* **2006**, *39*, 1328.
[15] C. Barner-Kowollik, M. Buback, B. Charleux, M. L. Coote, M. Drache, T. Fukuda, A. Goto, B. Klumperman, A. B. Lowe, J. B. Mcleary, G. Moad, M. Monteiro, R. D. Sanderson, M. P. Tonge, P. Vana, *J. Polym. Sci., Part A: Polym. Chem.* **2006**, *44*, 5809.
[16] H. Tobita, *Macromol. React. Eng.* **2008**, *2*, 371.
[17] H. Tobita, *Macromol. Symp.* **2008**, *261*, 36.
[18] R. G. Gilbert, "*Emulsion Polymerization: A Mechanistic Approach*", Academic Press, London **1995**.

